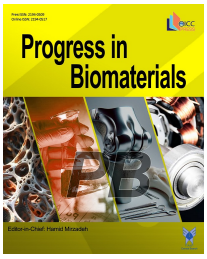

Volume 13, Issue 1, 132401 (1-12)

Progress in Biomaterials (PIBM)

https://doi.org/10.57647/pibm.2024.132401

Effect of Conductive Polymer, Magnetic Nanoparticles and Simvastatin Drug on Bone Regenaration in 3D Scaffolds Based on PGAZ-co-PEG$_{1000}$ and PLA

Rahele Samizadeh, Shahrokh Shojaei*, Soheila Zamanlui Benisi, Sadegh Rahmati, Milad Jafari-Nodoushan

Department of Biomedical Engineering, CT.C., Islamic Azad University, Tehran, Iran.

***Corresponding author:** shahrokhshojaei@iau.ir

Original Research

Received:
11 July 2023

Revised:
5 October 2023

Accepted:
19 November 2023

Published online:
30 March 2024

Abstract:

In this study, new 3D scaffolds based on synthesized PGAZ-co-PEG$_{1000}$ and PLA were prepared by salt leaching technique and Polythiophene as conductive pairs and Fe_2O_3 as magnetic nanoparticles, were also added to the 3D scaffolds. The FTIR test revealed that there is a relatively good interaction between the components used in these scaffolds. The XRD test also showed that the simultaneous presence of nanoparticles Fe_2O_3 and Polythiophene has a reducing effect on the crystal structure of the samples. SEM analysis also showed that suitable three-dimensional structures were formed within the samples and that the presence of other components in the scaffolds had significant effects on the three-dimensional structures of the scaffolds. The mechanical behavior of the samples in compression mode was analyzed in both dry and wet states. Young's modulus in dry and wet states showed completely different behavior among the samples. The compressive strength of the nanocomposite sample, which has twice the amount of nanoparticles as Polythiophene, was higher in both wet and dry states than in all the samples. Also, the degradation test was investigated in two acidic and basic pH, and interesting results were obtained. Alizarin red, H&E, and cell adhesion tests were performed on simple samples and samples loaded with the drug, and the results showed that the presence of Polythiophene and nanoparticles have a good effect on cell growth and proliferation, and Simvastatin drug has also demonstrated sound effects in addition to these substances.

Keywords: PGAZ-co-PEG$_{1000}$; Polythiophene; Salt leaching; Scaffolds

Cite this article: Samizadeh, R., Shojaei, S., Zamanlui Benisi, S., Rahmati, S., Jafari-Nodoushan, M. Effect of Conductive Polymer, Magnetic Nanoparticles and Simvastatin Drug on Bone Regenaration in 3D Scaffolds Based on PGAZ-co-PEG$_{1000}$ and PLA. *Progress in Biomaterials* **13**(1), Article 01 (2024).

1. Introduction

Tissue engineering is one of the best scientific fields, which is in close engagement with technical and medical sciences. In this area, there must be in-depth knowledge of materials science (Guo and Ma, 2014; Khademhosseini and Langer, 2016; Iravani and Varma, 2019). It should be determined what each material used in tissue engineering contributes to the achievement of the scaffold. Bone, as a prevalent tissue in the body of living organisms, has received much attention. On the other hand, this tissue is subject to much damage because it is considered a pillar for the internal organs of the body and plays a protective role against them (Chen et al., 2006; Charles-Harris et al., 2008; Venkatesan and Kim, 2014).

Recently, cell therapy or tissue engineering are commonly used to repair damaged tissues. The use of cell therapy has not been widely accepted due to its high cost and other problems (Farjaminejad et al., 2021; Golbaten-Mofrad et al., 2021; Hashemzadeh et al., 2021). In the meantime, tissue engineering is one of the most appropriate and best paths for doctors to treat patients due to its ease of use, affordable costs, and its ability to be used in many organs of the body. To prepare suitable and efficient scaffolds in tissue engineering, one must have a great deal of knowledge about biomaterials, their understanding, and, on the other hand, scaffold construction methods (Hosseini Chenani et

al., 2021; Tirgar et al., 2021; Asgharnejad-laskoukalayeh et al., 2022).
Among the materials used to make scaffolds used in tissue engineering, bio-polyesters have received much attention. These materials cover an extensive range, including PCL, PLA, etc (Zia et al., 2016; Bedian et al., 2017; Zhang et al., 2021). Petretta et al. prepare scaffolds based on PCL as the primary material and other materials such as bioactive glass. They concluded that these scaffolds, with the presence of such an additive, showed significant effects in repairing bone tissues (Petretta et al., 2021).
The use of conductive polymers in regenerative medicine has been proven, and many articles and research have been conducted in this field (Guo and Ma, 2018). Langer's research team investigated the presence of the conductive polymer polypyrrole on cell differentiation and showed that this polymer has outstanding effects on the growth and proliferation of stem cells into bone cells (Shastri et al., 1998). Sajesh and her colleagues made alginate conductive with the help of polypyrrole and then prepared a scaffold with chitosan and showed that the presence of conductive alginate in this scaffold had positive effects on the growth and proliferation of bone cells (Sajesh et al., 2013). Wu and her colleagues made gelatin conductive using polymer and then prepared a concluded hydrogels that using this conductive material enhances cell growth and differentiation in bone scaffolds (Wu et al., 2016). Polyglyceroazelaic acid is an important biopolyester material that has shown good effects in tissue engineering work and has been used in many biological activities. This material is obtained by a polycondensation process between alcoholic and acidic monosaccharides (Hosseini Chenani et al., 2021; Mohammadi et al., 2024).
In this study, a polymer of PGAZ-co-PEG_{1000} was synthesized using the polycondensation method, which has also been very limited in research on this material and has been mentioned in the only existing work by Mohammadi et al. (2024). After preparing this bio polyester, scaffolds were prepared by combining PLA and PGAZ-co-PEG_{1000} using the salt leaching method. Iron oxide nanoparticles and Polythiophene were also added to these scaffolds to increase their biological and other relevant properties. A wide variety of tests were performed on these scaffolds.

2. Materials and methods

2.1 Materials

A well-known company prepared all the chemical materials used in this study. PEG (with M_w = 1000 g/mol), PLA (granules with M_w = 84000 g/mol), and Fe_2O_3 nanoparticles with a fine particle size of 100 nm were purchased from Sigma Aldrich, USA. Other materials such as thiophene, Amoniom persulphate, NaCl particles (average particle size less than 200 microns), n-butane, hydrochloric acid (HCL), 1,4- dioxane and N, N-Dimethylmethanamide (DMF) with high purity were supplied from Merck. Co (Germany). Tin octanoate as catalyst was prepared from Sigma Aldrich Co. Hexamethylene diisocyanate (HDI) from Merck Co.

2.2 Sample preparation

In this study, all of the samples were prepared by salt leaching technique as well as the solution method. All of the stages of preparation of samples were presented briefly. In the first step, polymer PGAZ-co-PEG_{1000} must be synthesized. In this case, the monomers glycerin and Azelaic acid were reacted in a chemical reactor at 140 °C under vacuum for 48 hours. Then, a certain amount of polymer PEG_{1000} was added to it, and the reaction was carried out for another 48 hours under vacuum. After these steps, the resulting polymer is precipitated in n-butane and stored for the next step. To prepare Polythiophene, a certain amount of thiophene as the monomer is dispersed in water, then some hydrochloric acid (HCL) is added to it and stirred for 12 hours until the thiophene monomers are reactive. Then, an ammonium persulfate (APS) initiator is added to it and stirred for 24 hours; then, the brown precipitate is separated with filter paper and washed several times with water, and the resulting polymer is placed in an oven at 35 °C to dry completely and used in the following steps.
To prepare 3D scaffolds, first, 2 grams of polymer resin is dissolved in dioxane solvent for 5 hours at room temperature, then amounts corresponding to specific weight percentages of PLA polymer are added to the desired solution and stirred again for 12 hours. After this step, 0.001 cc of Tin(II) 2-ethyl hexanoate as a catalyst is added to the solution, the reaction temperature is increased to 50 degrees Celsius and stirred for 30 minutes. At this stage, two cc of HDI is added to the solution, and stirring is continued for 15 minutes, and then 40 times the weight of the polymers is poured into a beaker of salt and stirred vigorously with the polymer solution. This paste mixture is poured into molds and kept at room temperature for 2 weeks until they dry, and the crosslinking process is completed. Then, the samples are removed from the mold and placed in containers filled with distilled water until all their salts dissolve and are removed from them. After ensuring that all salts are removed, the samples are kept in an oven at 40 °C until they are dehydrated. To prepare samples containing nanoparticles and Polythiophene, first, specific weight amounts of these two materials are poured into 1,4 dioxane solvent and placed in an ultrasonic bath for 10 minutes to ensure that the particles are well dispersed. Then, the above process is continued to obtain nanocomposite scaffolds.
A summary of the sample fabrication process is graphically shown in Fig. 1. Table 1 details the percentage composition of the samples and the materials used in each sample.
The drug Simvastatin was used to aid osteogenesis in selected prepared scaffolds. In these scaffolds, the drug was loaded into scaffolds S1, S3, S4, and S6 based on specific protocols that exist in other studies Jin et al. (2021) and Ni et al. (2023).

2.3 Characterizations

The molecular structures of synthesized prepolymers were evaluated by proton Nuclear Magnetic Resonance (^{1}H NMR) and (^{13}C NMR) spectroscopy (NMR, AVANCE II-IHD400, Bruker). In the first step, all of the prepolymers were dissolved in a specific solvent (DMSO), their spec-

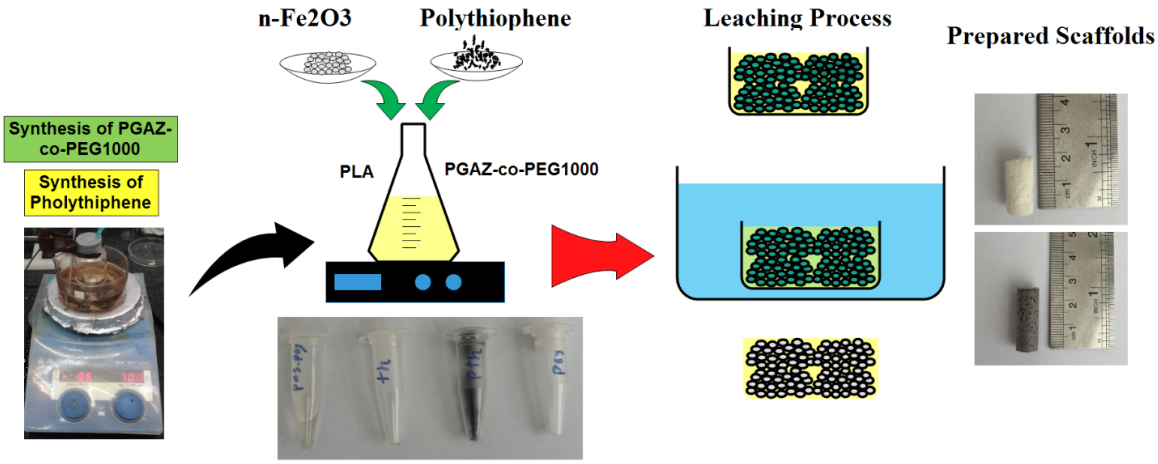

Figure 1. Prepared samples with leaching technique.

Table 1. Sample codes and their compositions.

Samples	PGAZ-co-PEG$_{1000}$	PLA (wt.%)	Pth (wt.%)	n-Fe$_2$O$_3$ (wt.%)
S1	100	-	-	-
S2	70	30	-	-
S3	70	30	5	-
S4	70	30	5	5
S5	70	30	10	5
S6	70	30	5	10

trums were recorded, and the obtained results were analyzed by using particular software.

Functional groups and the amount of interaction between the materials used were analyzed by Fourier Transform Infrared spectroscopy (FTIR, Lincoln FTIR instrument) range of $500-4000$ cm^{-1}. The characterization of chemical bonds in the solid scaffolds was evaluated by Attenuated Total Reflectance Fourier Transform Infrared (ATR-FTIR) mode.

The XRD analysis was accomplished using a diffractometer AWXD M300 within the scanning region of 2 h from 10° to 60°, with Cu-Kα radiation, for assessing the crystalline behavior of samples.

The molecular structures of synthesized prepolymers (r-PGAZ-co-Peg$_{1000}$) were evaluated by proton and Carbone Nuclear Magnetic Resonance (^{1}H-NMR, ^{13}C-NMR) spectroscopy (AVANCE IIIHD400, Bruker). At first, prepolymers were dissolved in a specific solvent, their spectrums were recorded, and the obtained results were analyzed by using particular software.

The morphology of the fractured surface of samples and the dispersion quality of bioactive glass (BG) nanoparticles into the polymeric matrixes were considered through a scanning electron microscope (SEM) Philips CM200. Mapping tools studied the dispersion and distribution of nanoparticles into polymeric matrixes for researching Calcium atoms (Ca) as the central element in the BG nanoparticles.

The thermal degradation behavior of prepared samples was studied using thermogravimetric analysis (TGA, STA449F3) in the inert atmosphere from room temperature to 600 °C with a heating rate of 10 °C /min.

A contact angle analysis was performed for all of the samples. A water drop was placed on smooth surfaces of polymeric films, and every 30 s, a photo was taken for 2 min. According to measuring right and left angles of water drop in each time can, be obtained hydrophilicity behavior of samples.

The hydrophilicity of all as-prepared scaffolds was measured using a sessile water drop method at room temperature. To achieve this goal, 2 µL of water was located on the surface of the scaffolds. The water droplets were then immediately photographed at determined time intervals (0 to 30 seconds). Using the imaging system, the static contact angles were calculated to determine the interaction between the water and the scaffold surface.

Hydrolytic degradation of samples was performed in 10 mL of phosphate buffer saline solution (PBS) as host milieu at 37 °C. Therefore, a specific size and weight of polymeric films (10 mm × 10 mm × 2 mm) were selected, and the weight loss of each sample was calculated as follows:

$$\text{Weight Loss } (\%) = \frac{W_0 - W_t}{W_0} \times 100 \qquad (1)$$

where W_0 is the initial weight of the sample particle, and W_t is the weight of the residual dried sample (after degradation) at each time (t; in the day).

The MTT assay was used for cell viability of the seeded

cells on cylindrical scaffolds on day 7 post-seeded. After 24, 72, and 120 hr of cell seeding, the media was changed with 200 µL MTT solution (0.5 mg/mL, Sigma) and incubated to form formazan crystals for four hr. After the incubation period, 200 µL dimethyl sulfoxide (DMSO, Sigma) was added to dissolve the blue formazan crystals in a dark room for 15 min by shaking. The absorbance of each sample (n = 3) was then measured at 570 nm using an ELIZA reader (Expert 96, Asys Hitch, Ec Austria).

The SEM was used for the investigation of morphology and attachment of the seeded cells on scaffolds after 5 days of the culture period. The seeded cells on samples were fixed with 2% paraformaldehyde and 2.5% glutaraldehyde for 90 min at 27 °C. The samples were then rinsed two times in PBS and dehydrated with increasing concentrations of ethanol (30, 50, 70, 85, 90, and 100%) for 5 min. Finally, the samples were prepared to see using SEM by sputter coating with gold.

Alizarin Red analysis was performed to characterize the mineralization (Calcium on the surface of scaffolds). MC3T3-E1 and BMSc cells were seeded on the samples and were cultured for 3, 8, and 11 days in an incubator at 37 °C and 5% CO_2. Media was removed, and cells were fixed using 4% PFA for 14 min. Samples were stained using 1% Alizarin Red powder in PBS for 45 min and then were rinsed with PBS solution before imaging under a fluorescence microscope (Zeiss Axio Observer Z1, Zeiss, USA).

All data were represented as mean ± SD. A one-way analysis of variance (one-way ANOVA) and Tukey's posthoc test using GraphPad Prism software was applied. Significance levels were set at $p < .05$.

3. Results and discussion

3.1 Determining the prepolymer structure and examining the interactions in scaffolds

Determining the structure of the synthesized polymer is one of the most critical parts of this research. Using analyses ^{1}H-NMR and ^{13}C-NMR, the structure of the r-PGAZ-co-PEG_{1000} can be easily determined. Accordingly, the results of these tests are shown in Fig. 2. The chemical analysis of the groups in PGAZ material was presented in Fig. 2 (A,C) as follows:

^{1}H-NMR (499 MHz, DMSO) δ 14.41 (d, J = 13.9 Hz, 50H), 14.41 (d, J = 13.9 Hz, 39H), 5.28 (dd, J = 205.3, 167.2 Hz, 39H), 4.91 (d, J = 27.1 Hz, 8H), 4.97 - 4.74 (m, 14H), 4.97 – 4.64 (m, 18H), 4.97 – 4.16 (m, 42H), 4.16 – 3.76 (m, 52H), 3.61 (dd, J = 10.6, 5.3 Hz, 5H), 3.59 – 3.23 (m, 37H), 3.12 – 1.97 (m, 80H), 1.48 (d, J = 5.8 Hz, 77H), 1.23 (s, 121H).

^{13}C-NMR (126 MHz, dmso) δ 41.15 – 40.45 (m), 40.29 (d, J = 19.2 Hz), 40.21 – 39.43 (m), 34.39 – 34.16 (m), 34.16 – 33.64 (m), 28.78 (d, J = 14.1 Hz), 24.97 – 24.26 (m).

In these results, the associated peaks of CH_2 for Azelaic acid groups are clear (Fig. 2 (B,D)). The results analysis of the results sample of PGAZ-co-PEG_{1000} are as follows:

^{1}H-NMR (499 MHz, DMSO) δ 4.74 – 4.17 (m, 3H), 4.17 – 3.17 (m, 231H), 3.71 – 3.17 (m, 212H), 3.71 – 2.79 (m, 207H), 2.36 – 2.13 (m, 27H), 1.43 (dd, J = 55.8, 48.3 Hz, 29H), 1.24 (s, 42H).

^{13}C-NMR (126 MHz, dmso) δ 174.91 (d, J = 3.5 Hz), 40.38 (s), 40.21 (s), 40.17 – 39.43 (m), 34.05 (s), 33.81 (s), 28.84 (t, J = 11.6 Hz), 24.86 (d, J = 5.6 Hz).

The PEG's groups have been appropriately placed in the structure. The differences in the peaks between the PGAZ and PGAZ-co-PEG_{1000} demonstrate the presence of PEG's

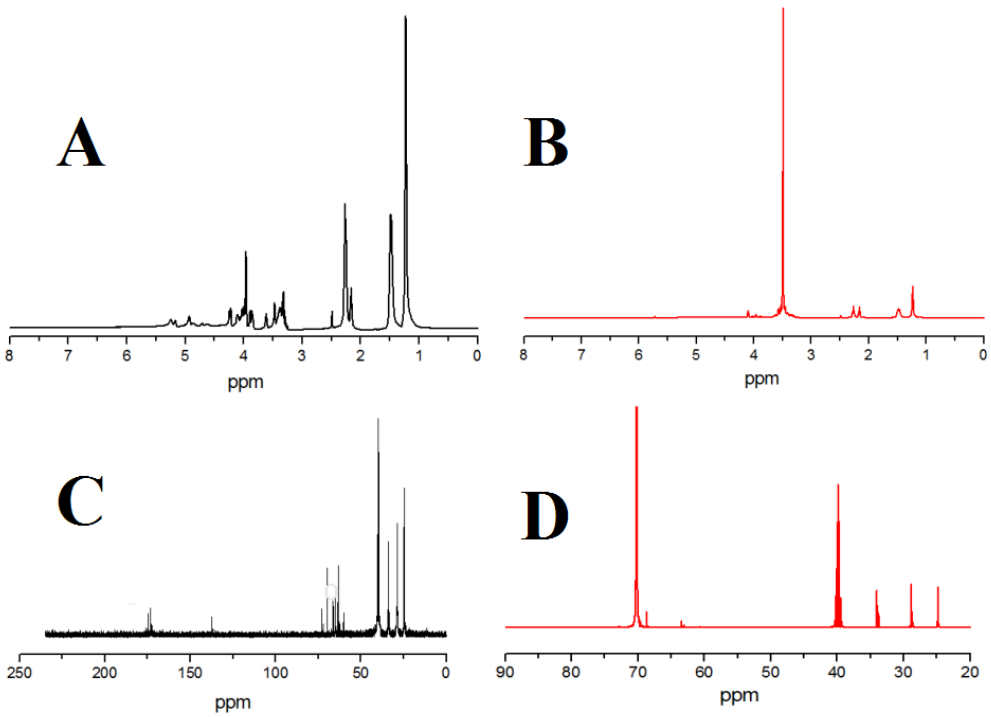

Figure 2. HNMR and CNMR of synthesized polymer: (A, C) PGAZ and (B, D) PGS-co-PEG_{1000}.

groups (Rostamian et al., 2020; Rostamian et al., 2022). To better understand the interaction between the materials used, Fig. 3 (A) initially shows the FTIR results from S1, S2, and S3 samples. The spectrum of sample S1 showed that the functional groups related to polyesters were visible in this sample, and in sample S2, with the presence of 30% by weight of PLA, very slight changes were seen in the important groups of this sample. However, in sample S3, with the presence of 5% by weight of Polythiophene, very significant changes were seen in the spectrum of this sample. This observation is related to the interaction of the sulfur heterocyclic in Polythiophene with the hydrogen bonds in the ester and hydroxyl groups in the polymer chain PGAZ-co-PEG_{1000}. The results of FTIR analysis between samples in which the weight percentage of Polythiophene and n-Fe_2O_3 varies were examined and presented in Fig. 3 (B). Figure 3 (C) shows the X-ray analyses of all of the samples. Based on the reported results, it can be seen that most of the peaks in this analysis are visible at angles of 20° to 25°. This behavior is also mainly related to PGAZ-co-PEG_{1000}, which, based on the results of previous reports, has shown peaks in this region that are related to the crystal structures in their polymeric families. The highest crystalline structure is seen in S1, and the lowest crystallinity is seen in samples 2 and 3, which is due to the presence of Polythiophene and Fe_2O_3 in it and the disruption of order in the base polymer.

3.2 Microstructures, EDX, and mapping analysis

In Fig. 4, the microstructures of all of the prepared samples have been analyzed in two different magnifications. In the pure sample (Fig. 4 (A,A′)), it is observed that suitable pores have been created, a good three-dimensional structure is seen in this sample, and the boundaries between the pores are completely defined and clear. In sample S2, with the presence of 30% by weight of PLA, the three-dimensional structures have slightly changed, and compared to S1, the structural order in this sample has decreased (Fig. 4 (B,B′)). Morphological images of sample S3 are given in Fig. 4 (C,C′). In these images, it can be seen that the presence of 5% by weight of Polythiophene has slightly changed the structure of the sample, and particles can be seen next to the walls of the pores, which are most likely related to this polymer material. In sample S4, both additives exist together in equal proportions (5 wt.%), and their role in the changes in the morphology of the sample can be seen in Fig. 4 (D,D′).

In sample S5, the presence of Polythiophene is about twice as high as n-Fe_2O_3, and morphological changes in this sample are shown in Fig. 4 (E,E′). In these figures, it can be seen that the pore structures in this sample have been slightly deformed and have become circular. In the morphology of sample S6, the ratio of nanoparticles to Polythiophene is higher, and it is also observed that the three-dimensional

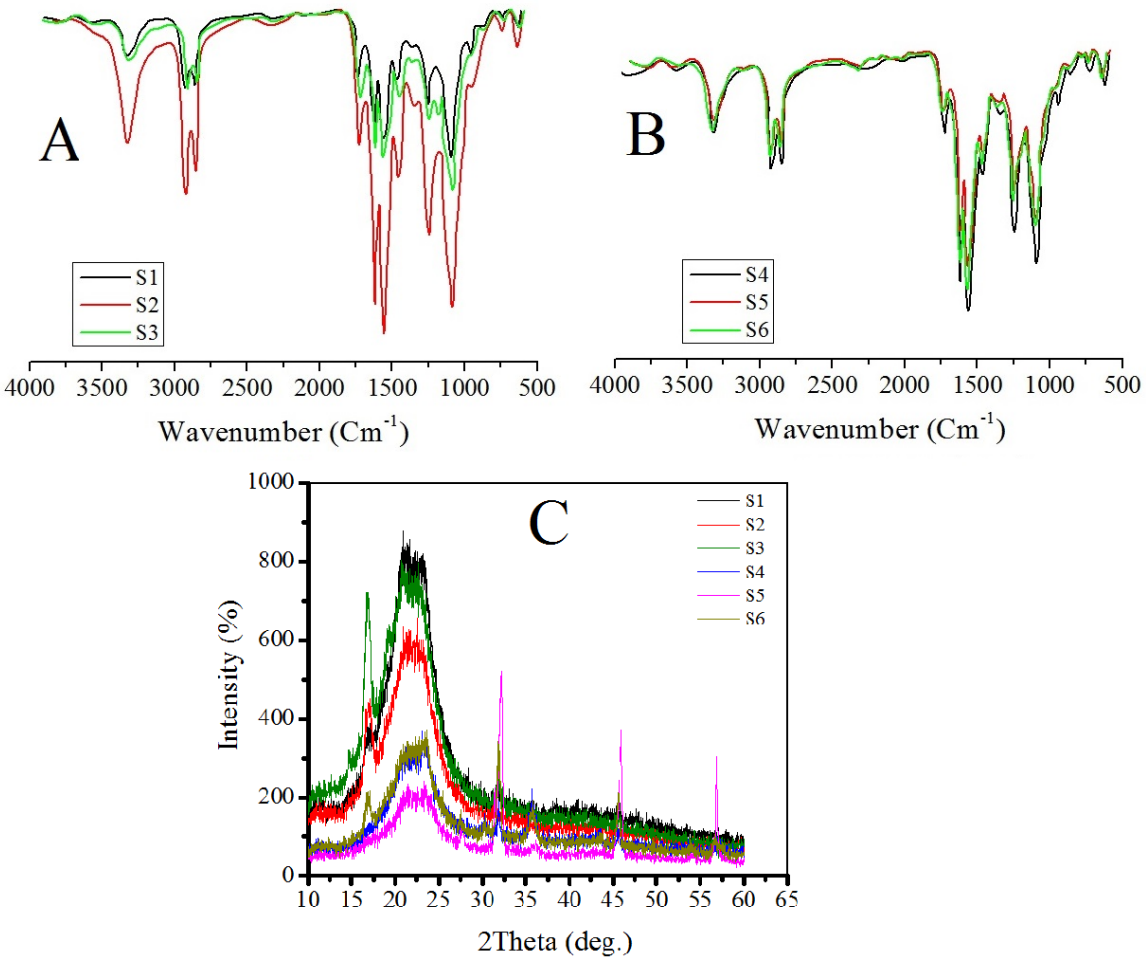

Figure 3. FTIR and XRD analysis of studied samples.

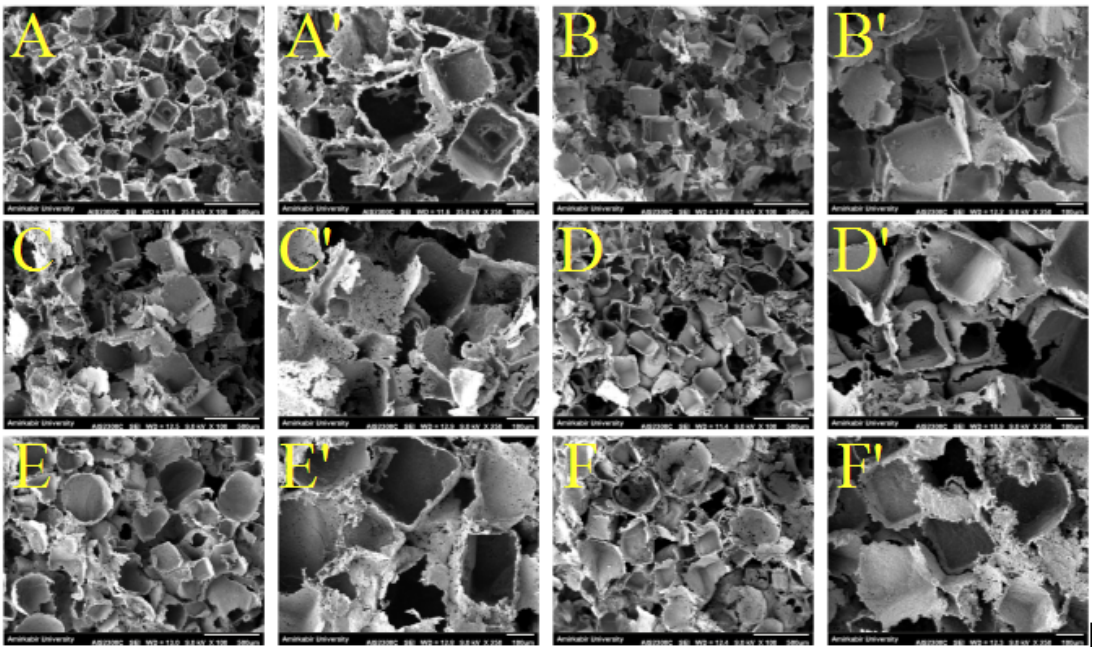

Figure 4. SEM analysis of studied samples at different magnifications: (A, A′) S1, (B, B′) S2, (C, C′) S3, (D, D′) S4, (E, E′) S5 and (F, F′) S6.

structure has become irregular and is similar to sample S5. Perhaps the reason for this morphology is the increased hydrophilicity in these samples and better interaction between polymer materials.

The dispersion of Polythiophene and Fe_2O_3 nanoparticles within the 3D scaffolds was investigated using EDX and mapping analysis, and their results are shown in Fig. 5 for the samples specified. In sample S3, the dispersion of sulfur atoms in the sample indicates that a relatively good interaction has been created between polymers Polythiophene and PGAZ-co-PEG_{1000}, which has been able to show this proper dispersion. It was also observed in samples S4, S5, and S6 that the dispersion of iron nanoparticles next to Polythiophene was appropriate, and these atoms could be seen everywhere in the sample, confirming the proper interaction between the components and the appropriate mixing process for making the samples.

3.3 Mechanical analysis

In this section, the mechanical analysis of all of the prepared samples in dry and wet conditions was analyzed, and their results have been presented in Fig. 6. In Fig. 6 (A), strain-stress curves of samples in dry conditions were presented. In this figure, it can be seen that the mechanical behavior of the samples can be divided into two categories based on the location of sample S1. In almost all samples, the mechanical behavior is below the curve of sample S1. Based on this, it can be concluded that the addition of PLA has reduced the mechanical properties of the sample. This observation is likely due to the weak interaction between the two primary materials used in this study (Hassanajili et al., 2019; Wang et al., 2021; Davoodi et al., 2022).

Meanwhile, the mechanical behavior of sample S6 was interesting. In this sample, the proportion of nanoparticles was twice that of Polythiophene, which was able to provide a better structure and increase the compressive strength of the sample. This behavior can be partly attributed to the three-dimensional structure of the scaffold in the SEM images.

The mechanical properties of prepared samples were also investigated in wet conditions, and their results are presented in Fig. 6 (B). In this figure, the difference in mechanical behavior between the samples and sample S1 has increased, and sample S6 still has mechanical properties under these conditions, which is due to the well-formed structure in this sample. The modulus and compressive strength of the samples in both dry and wet conditions are compared in Fig. 6 (C,D). In the dry state, most of the compressive modulus is related to samples S4 and S6, and overall, the compressive modulus is higher for samples in which nanoparticles and Polythiophene were used compared to other samples. However, in the wet state, the opposite trend was observed compared to the dry state. In this condition, the modulus of samples S1 and S3 was higher than that of the other samples. The compressive strength analysis of the samples in wet and dry conditions is shown in Fig. 6 (D). In the dry state, the compressive strength of the samples in which the additive was used is higher. In wet conditions, these samples also have higher compressive strength, indicating structural strengthening of these samples.

3.4 Electrical conductivity

Electrical conductivity is a vital property for the investigation properties of conductive scaffolds. The electrical properties of all samples were examined, and their results are presented in Table 2. Based on the data obtained, it is clear that in sample number 3, the electrical conductivity increased with the addition of Polythiophene. In sample number 4, the electrical conductivity has improved with the addition of iron nanoparticles. The reason for this result could be due to the presence of iron nanoparticles and the creation of a synergistic state between Polythiophene. It is

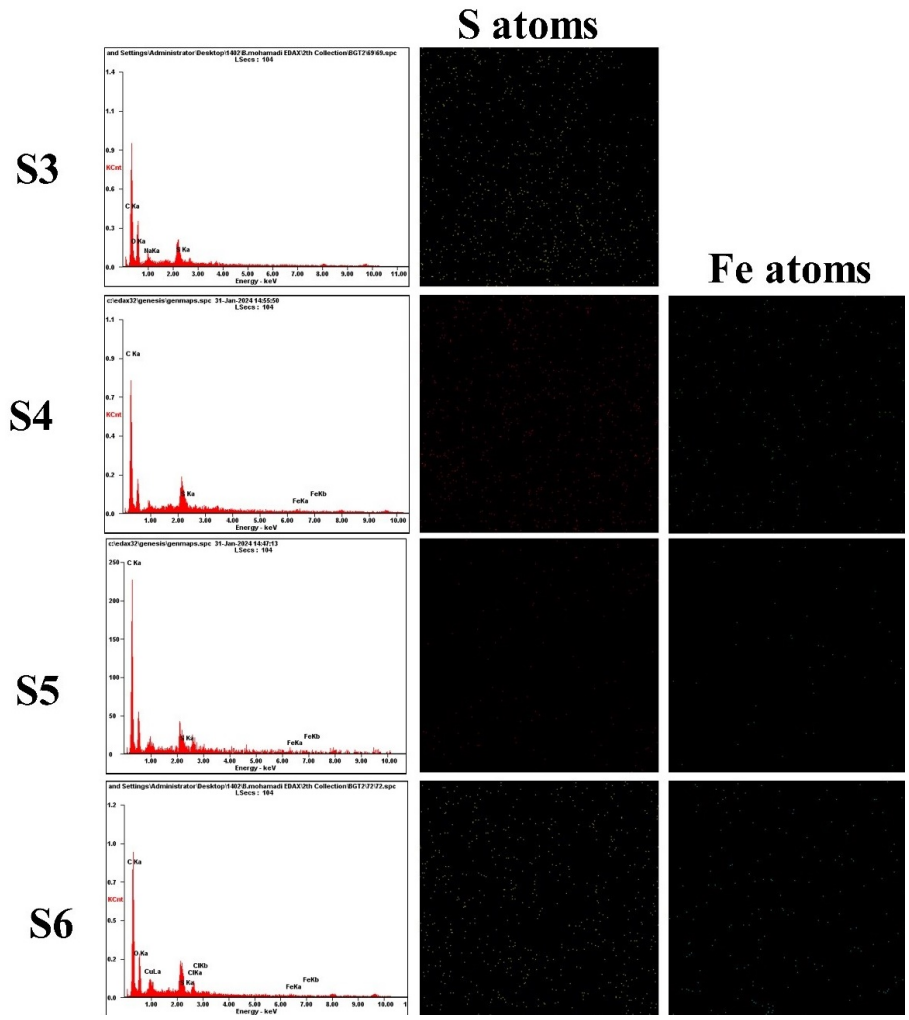

Figure 5. EDX and Mapping analysis of studied samples.

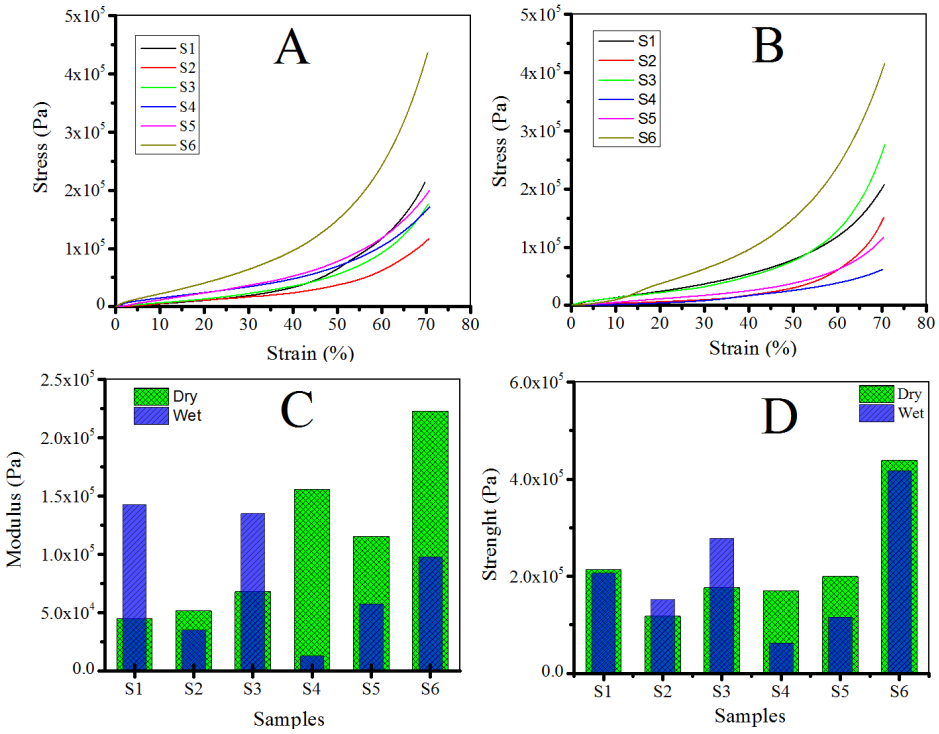

Figure 6. Mechanical analysis of studied samples: Strain and stress: (A) dry and (B) wet and Modulus (C) and Strength (D).

Table 2. Electrical conductivity of studied samples.

Samples	Specific resistance (Ω/cm)
S1	3063052.8
S2	997589.8
S3	1702664.5
S4	2191408.2
S5	3907044.2
S6	4364309.9

observed that with increasing the weight percentage ratio of Polythiophene to nanoparticles, there are no drastic changes in the electrical conductivity of the scaffolds. This behavior may be due to the presence of the nature of both additives in the samples.

3.5 Degradation analysis

The results of the degradability test were performed for all samples prepared in two conditions (pH = 7 and pH = 12), and their results over a period of 60 days are shown in figure 7. In both situations, it has been determined that the degradation rate in S1 is higher than in the other samples. This analysis is also related to the PEG blocks present in the polymer chain structure of this sample, which cause interactions with ions that have a significant impact on the destruction of ester bonds (Chen et al., 2010; Aghajan et al., 2020; Sood et al., 2021). S6 also showed less degradation behavior in both cases, which is due to the presence of twice the amount of iron nanoparticles compared to the Polythiophene polymer. These particles, by creating an interconnected structure, prevent the penetration of oxidizing agents into the polymer chains and, on the other hand, reduce the degradation rate.

3.6 MTT, Alizarin Red, and H&E staining analysis

The results of the cytotoxicity test for all prepared samples are given in figure 8 for the three selected times. In this figure, it can be seen that at 24 hours, the cytotoxicity behavior of the samples is not stable. After 48 hours, the behavior becomes slightly more stable, and the samples containing nanoparticles and Polythiophene show good behavior. After 72 hours, S6 showed less cytotoxicity compared to the other samples. In this section, the amount of calcium pyrophosphate crystals was measured using the Alizarin red test, and the morphology of cells on the surface of the scaffolds was examined using the H&E analysis, and their results are also presented in this figure.

The drug Simvastatin was loaded on samples S1 and S3, and its effect was investigated in this section. Based on the results shown in figure 8, it can be seen that the pure sample showed a lower amount of calcium crystallinity than the sample containing 5% by weight of Polythiophene. The reason for this observation may be related to the greater exchange of ions on the surface of scaffold S2, which leads to better growth of the cells used and greater accumulation of calcium on the surface of this sample (Mahdavi et al., 2024). In these two samples, it can also be seen that scaffold S2 also showed better behavior in the presence of the drug, which is probably due to better interaction between the drug and Polythiophene.

In sample number S4, 5% by weight of iron nanoparticles was added to the scaffold along with Polythophene, and the results showed that the presence of these two materials together created a suitable structure and the ability of calcium deposition in this sample was increased (Fig. 8 (C)) in compare with previous samples. Also, the presence of

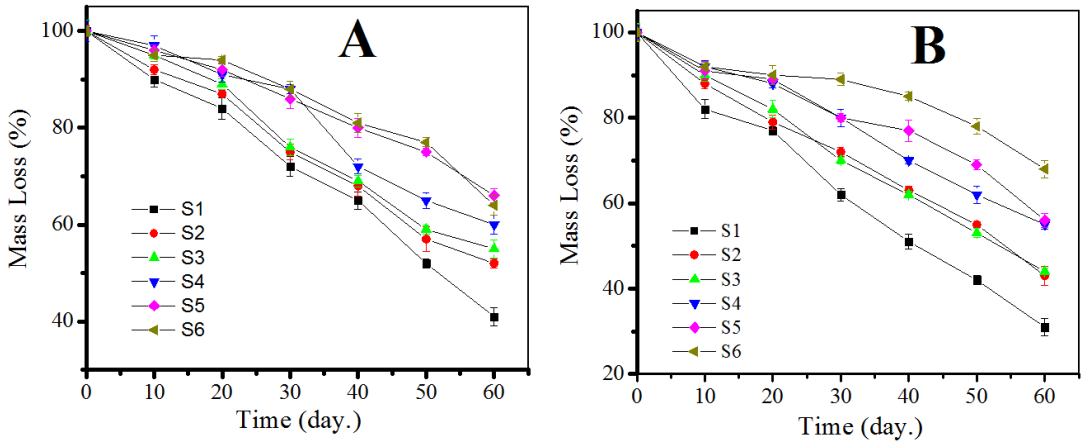

Figure 7. Degradation analysis for studied samples: (A) pH = 7 and (B) pH = 12.

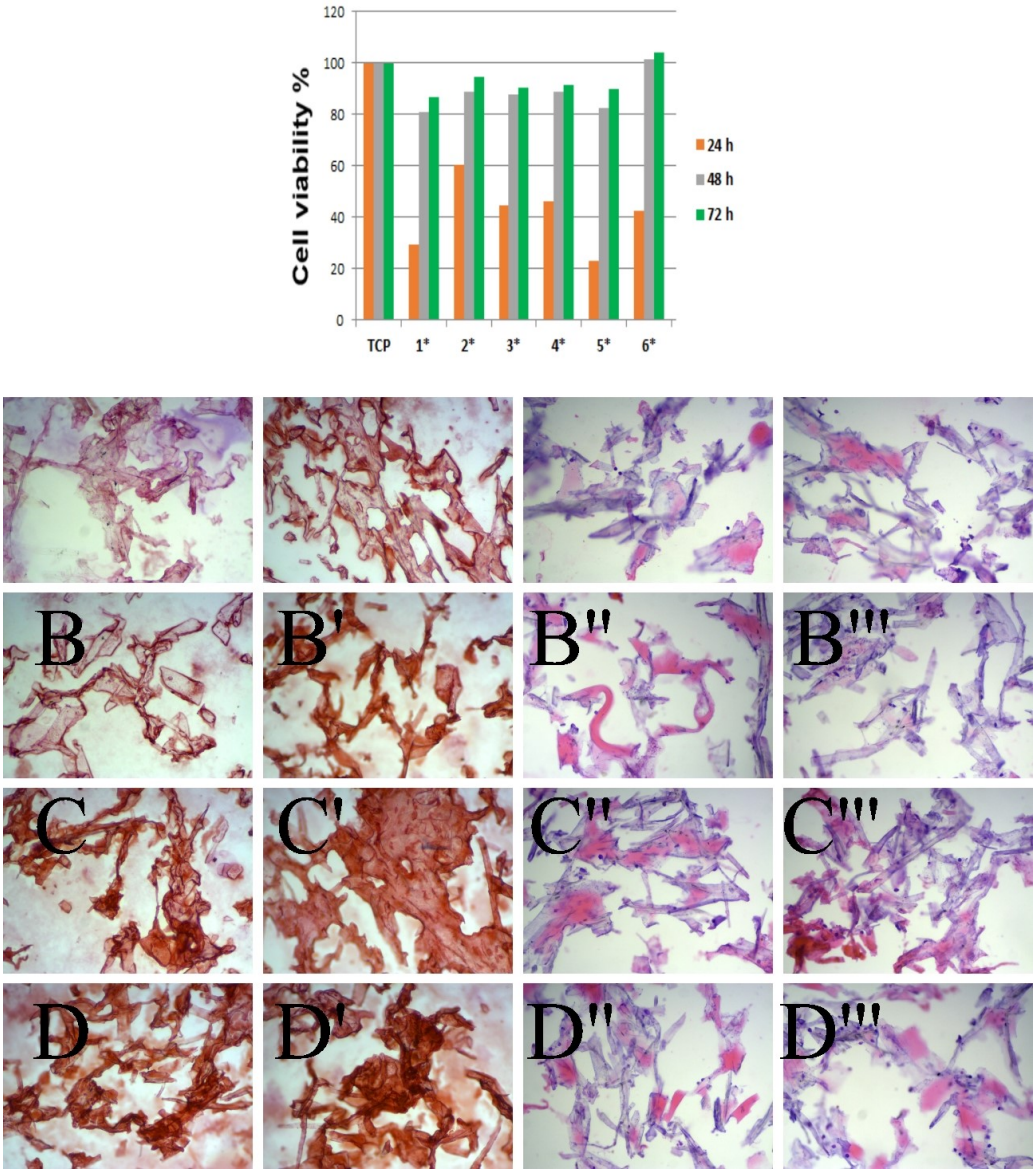

Figure 8. MTT, Alizarin Red and H&E for studied samples (A, A′) S1 and S1+Druge, (B, B′) S3 and S3+Drug, (C, C′) S4 and S4+Drug and (D, D′) S6 and S6+Drug, H&E analysis (A″, A‴) S1 and S1+Drug, (B″, B‴) S3 and S3+Drug, (C″, C‴) S4 and S4+Drug and (D″, D‴) S6 and S6+Drug.

the drug in this sample has covered a much larger surface area of the sample with calcium crystals (Fig. 8 (C′)). In sample S6, the weight percentage of iron nanoparticles was twice that of Polythiophene, which showed that it had a very high impact on this test compared to other samples; it can be seen that the area of colored areas in this sample have increased (Fig. 8 (D)). Also, the presence of the drug in this sample has shown greater effects compared to other samples (Fig. 8 (D′)).

In the pure sample, it is observed that the morphology of the cells is in good condition, and the level of collagen produced in this sample is low (Fig. 8 (A″,A‴)). With the presence of 5% by weight of Polythiophene and also the drug in sample S2, the morphology of the cells is suitable, and in this sample, the level of collagen prepared is better than sample S1 (Fig. 8 (B″,B‴)). In sample S3, the presence of nanoparticles and Polythiophene had outstanding effects on the cells, and in addition, the presence of the drug also showed a positive impact on the formation of cell morphology (Fig. 8 (C″,C‴)). In sample S6, with the presence of more nanoparticles in the sample, there was a slight decrease in cell morphology compared to sample S4, and on the other hand, the presence of the drug also showed slight effectiveness (Fig. 8 (D″,D‴)).

3.7 Cell attachments

In this section (Fig. 9), the number of cell adhesions on the surface of selected scaffolds at 3, 5, and 7 days was presented, and the role of Polythiophene, n-Fe_2O_3, and drug on cell adhesion was investigated. In the pure sample, it is observed that the presence of the drug in this sample increases the amount of cell interaction with the scaffold surface, and on the other hand, proper adhesion is also observed between the cell and the scaffold. Also, over several days, the amount of cells has increased, which has shown the good cell growth effect of this scaffold. In sample S3, the presence of Polythiophene has demonstrated effects in the sample and has created a high level of adhesion in the sample, which may

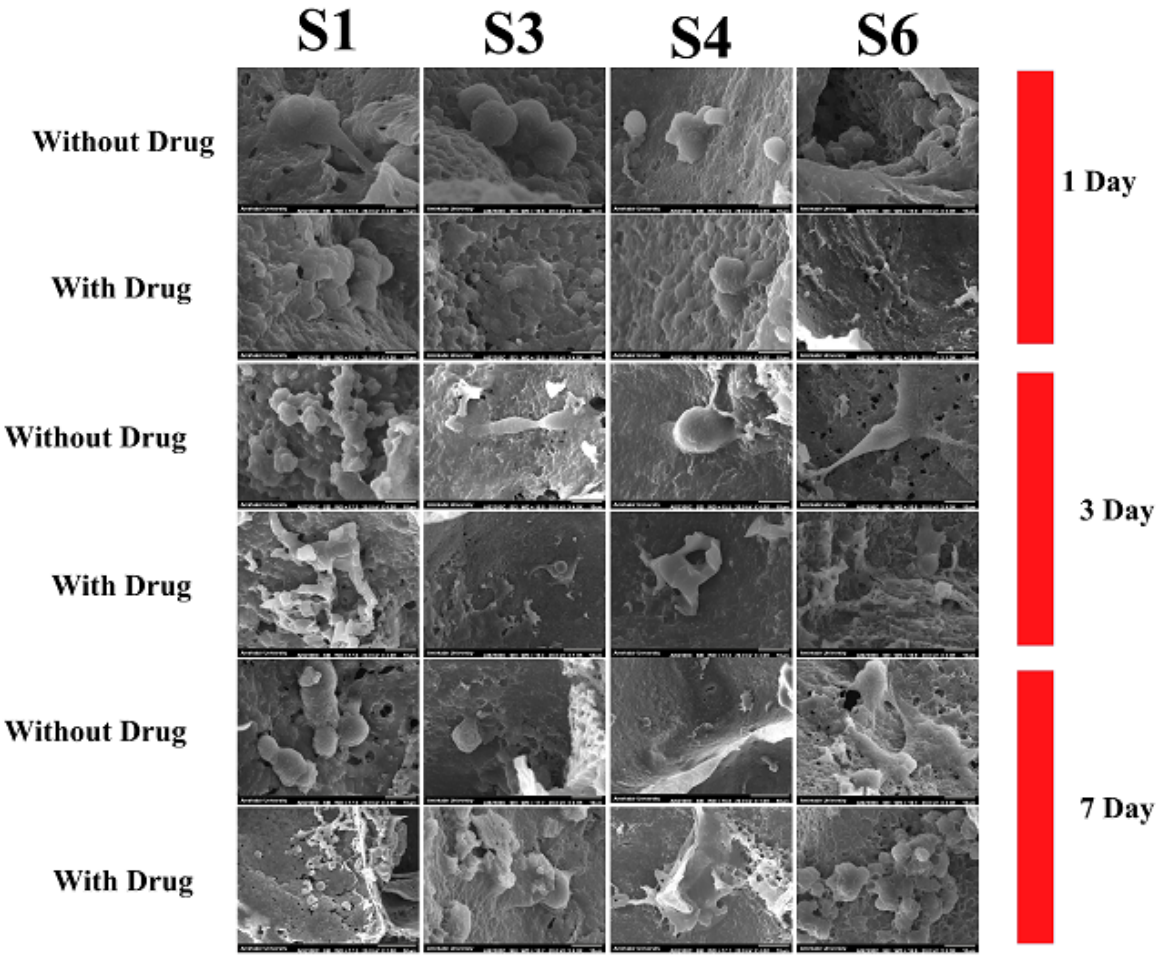

Figure 9. SEM of cell attachment from scaffolds without and with drug at different times.

be due to better exchange of nutrients in this sample due to the presence of the conductive polymer Polythiophene. On the other hand, it is observed that the presence of the drug in this sample has also shown a good role in cell adhesion and growth and proliferation of cells over the specified period. In sample S4, the presence of nanoparticles alongside Polythiophene, with an equal weight percentage, has shown a good role in the adhesion rate, and the drug has also had sound effects on the growth and proliferation of cells. In sample S6, as the weight percentage of iron nanoparticles increased, the presence of cells on the scaffold increased, and it was also observed that the role of the drug in this sample became more pronounced and caused greater cell proliferation in this sample (Golbaten-Mofrad et al., 2021; Hosseini Chenani et al., 2021).

4. Conclusion

In this study, 3D scaffolds based on PGAZ-co-PEG_{1000} were prepared by combining materials PLA, Polythiophene, and Fe_2O_3 as nanoparticles using the salt leaching method. In the construction of 3D scaffolds, the weight percentage ratio between PGAZ-co-PEG_{1000} and PLA was kept constant (70/30), and the presence of Polythiophene and n-Fe_2O_3 within the prepared samples was determined in the different weight fractions. ^{1}H-NMR and ^{13}C-NMR were used to prove the accurate synthesis of PGAZ-co-PEG_{1000}, and the results showed that the polycondensation method successfully synthesized the original polymer used in this study. Using a solution method and various materials, different three-dimensional scaffolds were prepared in this research, and a wide variety of tests were used to examine the physical, mechanical, and biological properties of these scaffolds. Using FTIR testing, it was determined that there were relatively good interactions between the components used in the scaffolds and that the ester groups created good interactions with the active groups on the surface of the nanoparticles and Polythiophene, which perhaps confirms the good compatibility between these materials used in this research.

The results of XRD analysis showed that a semi-crystalline structure was observed in all samples, and mainly one type of crystal structure was present. On the other hand, the presence of additives in the samples severely weakened the crystal structures. The microstructures in the prepared samples were observed using SEM, and the results showed that a good structure was mainly achieved within all samples using the salt leaching process. The dispersion of sulfur atoms and iron atoms, which was a measure of the dispersion of Polythiophene materials and iron nanoparticles within the prepared scaffolds, was investigated using a mapping test, and the results showed that in any

percentage combination between these two materials, the dispersion of these particles within the prepared scaffolds was completely optimal. In the dry state, the compressive modulus of sample 1 and sample 3 is higher than the other samples. The presence of nanoparticles along with Polythiophene has reduced the compressive modulus of the samples, which may be due to the creation of more porosity in the samples. In wet conditions, sample number 6 has a higher compressive modulus compared to other samples, and its compressive modulus is even higher than in the dry state, which may be due to the creation of a porous structure in this sample and the placement of nanoparticles and suitable Polythiophene polymer among the porous structures of the sample. Also, the compressive strength of the samples showed that sample number 6 had higher compressive strength than all samples in both wet and dry states. Electrical property testing also revealed that the presence of Polythiophene and iron nanoparticles created a good conductive structure in the scaffolds.

The contact angle test also showed that all samples have suitable hydrophilicity, and the tendency to absorb water is higher within all samples. Degradability tests were conducted for all samples in both acid and alkaline conditions over 60 days, and the results showed that sample S1 had the highest rate of degradation. The presence of Polythiophene and iron nanoparticles affected the rate of degradation in the samples, and sample S6, which has a higher percentage of nanoparticles, had the lowest degradation rate in both conditions. Cytotoxicity tests were performed on the samples over specific periods, and the results showed that all samples showed good behavior over 48 and 72 hours. To see better effects on bone cell growth, the drug Simvastatin was also used in some scaffolds, and Alizarin Red and H&D tests were performed on the samples, and it was found that samples containing 10% by weight of iron nanoparticles and 5% by weight of Polythiophene showed better results and on the other hand, the drug also intensified the effects. Cell adhesion tests were also performed on the specified scaffolds, and it was observed that due to the appropriate hydrophilicity of the scaffolds and the creation of relatively rough surfaces on the scaffolds, the level of cell adhesion on them was relevant, and the presence of the drug also enhanced this adhesion.

Authors contributions
Authors have contributed equally in preparing and writing the manuscript.

Availability of data and materials
The data that support the findings of this study are available from the corresponding author, upon reasonable request.

Conflict of interests
The authors declare that they have no known competing financial interests or personal relationships that could have appeared to influence the work reported in this paper.

References

Aghajan M. H., Panahi-Sarmad M., Alikarami N., et al. (2020) Using solvent-free approach for preparing innovative biopolymer nanocomposites based on PGS/gelatin. *Eur Polym J* 131
DOI: https://doi.org/10.1016/j.eurpolymj.2020.109720.

Asgharnejad-laskoukalayeh M., Golbaten-Mofrad H., Zamanlui S. (2022) Preparation and characterization of a new sustainable bio-based elastomer nanocomposites containing poly(glycerol sebacate citrate)/chitosan/n-hydroxyapatite for promising tissue engineering applications. *J Biomater Sci Polym Ed* 33:2385–2405.
DOI: https://doi.org/10.1080/09205063.2022.2104600.

Bedian L., Villalba-Rodríguez A. M., Hernández-Vargas G., et al. (2017) Bio-based materials with novel characteristics for tissue engineering applications – A review. *Int J Biol Macromol* 98:837–846.
DOI: https://doi.org/10.1016/j.ijbiomac.2017.02.048.

Charles-Harris M., Koch M. A., Navarro M., et al. (2008) A PLA/calcium phosphate degradable composite material for bone tissue engineering: an in vitro study. *J Mater Sci Mater Med* 19:1503–1513.
DOI: https://doi.org/10.1007/s10856-008-3390-9.

Chen Q. Z., Ishii H., Thouas G. A., et al. (2010) An elastomeric patch derived from poly(glycerol sebacate) for delivery of embryonic stem cells to the heart. *Biomaterials,*
DOI: https://doi.org/10.1016/j.biomaterials.2010.01.108.

Chen Q. Z., Thompson I. D., Boccaccini A. R. (2006) 45S5 Bioglass®-derived glass-ceramic scaffolds for bone tissue engineering. *Biomaterials* 27:2414.

Davoodi B., Goodarzi V., Hosseini H., et al. (2022) Design and manufacturing a tubular structures based on poly(ε-caprolactone)/poly(glycerol-sebacic acid) biodegradable nanocomposite blends: suggested for applications in the nervous, vascular and renal tissue engineering. *J Polym Res* 29:1–15.
DOI: https://doi.org/10.1007/S10965-021-02881-8.

Farjaminejad S., Shojaei S., Goodarzi V., et al. (2021) Tuning properties of bio-rubbers and its nanocomposites with addition of succinic acid and ε-caprolactone monomers to poly(glycerol sebacic acid) as main platform for application in tissue engineering. *Eur Polym J* 159:110711. DOI: https://doi.org/10.1016/j.eurpolymj.2021.110711.

Golbaten-Mofrad H., Seyfi Sahzabi A., Seyfikar S., et al. (2021) Facile template preparation of novel electroactive scaffold composed of polypyrrole-coated poly(glycerol-sebacate-urethane) for tissue engineering applications. *Eur Polym J* 159:110749.
DOI: https://doi.org/10.1016/j.eurpolymj.2021.110749.

Guo B., Ma P. X. (2018) Conducting Polymers for Tissue Engineering. *Biomacromolecules* 19:1764–1782.
DOI: https://doi.org/10.1021/acs.biomac.8b00276.

——— (2014) Synthetic biodegradable functional polymers for tissue engineering: A brief review.

Hashemzadeh M. R., Taghavizadeh Yazdi M. E., Amiri M. S., Mousavi S. H. (2021) Stem cell therapy in the heart: Biomaterials as a key route. *Tissue Cell* 71:101504.
DOI: https://doi.org/10.1016/j.tice.2021.101504.

Hassanajili S., Karami-Pour A., Oryan A., Talaei-Khozani T. (2019) Preparation and characterization of PLA/PCL/HA composite scaffolds using indirect 3D printing for bone tissue engineering. *Mater Sci Eng C* 104:109960.
DOI: https://doi.org/10.1016/j.msec.2019.109960.

Hosseini Chenani F., Rezaei V. F., Fakhri V., et al. (2021) Green synthesis and characterization of poly(glycerol-azelaic acid) and its nanocomposites for applications in regenerative medicine. *J Appl Polym Sci* 138:50563. DOI: https://doi.org/10.1002/app.50563.

Iravani S., Varma R. S. (2019) Plants and plant-based polymers as scaffolds for tissue engineering. *Green Chem* 21:4839–4867.
DOI: https://doi.org/10.1039/C9GC02391G.

Jin H., Ji Y., Cui Y., et al. (2021) Simvastatin-Incorporated Drug Delivery Systems for Bone Regeneration.. *ACS Biomater Sci Eng* 7:2177–2191.
DOI: https://doi.org/10.1021/acsbiomaterials.1c00462.

Khademhosseini A., Langer R. (2016) A decade of progress in tissue engineering. *Nat Protoc* 11:1775–1781.
DOI: https://doi.org/10.1038/nprot.2016.123.

Mahdavi R., Zahedi P., Goodarzi V. (2024) Application of Poly(Glycerol Itaconic Acid) (PGIt) and Poly(ε-caprolactone) Diol (PCL-diol) as Macro Crosslinkers Containing Cloisite Na^+ to Application in Tissue Engineering. *J Polym Environ,* 1–15.
DOI: https://doi.org/10.1007/S10924-023-03162-9/METRICS.

Mohammadi A., Salimi A., Goodarzi V., et al. (2024) Synthesis and Characterization of PEGylated Poly(Glycerol Azelaic Acid) and Their Nanocomposites for Application in Tissue Engineering. *J Polym Environ* 1-17
DOI: https://doi.org/10.1007/S10924-024-03194-9/METRICS.

Ni Q., Zhu J., Li Z., et al. (2023) Simvastatin promotes rat Achilles tendon-bone interface healing by promoting osteogenesis and chondrogenic differentiation of stem cells. *Cell Tissue Res* 391 (10.1007/s00441-022-03714-w): 339–355.

Petretta M., Gambardella A., Boi M., et al. (2021) Composite Scaffolds for Bone Tissue Regeneration Based on PCL and Mg-Containing Bioactive Glasses. *Biology (Basel)* 10

Rostamian M., Hosseini H., Fakhri V., et al. (2022) Introducing a bio sorbent for removal of methylene blue dye based on flexible poly(glycerol sebacate)/chitosan/graphene oxide ecofriendly nanocomposites. *Chemosphere* 289:133219.
DOI: https://doi.org/10.1016/j.chemosphere.2021.133219.

Rostamian M., Kalaee M. R., Dehkordi S. R., et al. (2020) Design and characterization of poly(glycerol-sebacate)-co-poly(caprolactone) (PGS-co-PCL) and its nanocomposites as novel biomaterials: The promising candidate for soft tissue engineering. *Eur Polym J* 138 (10.1016/J.EURPOLYMJ.2020.109985): 109985.

Sajesh K. M., Jayakumar R., Nair S. V., Chennazhi K. P. (2013) Biocompatible conducting chitosan/polypyrrole–alginate composite scaffold for bone tissue engineering. *Int J Biol Macromol* 62:465–471.
DOI: https://doi.org/10.1016/j.ijbiomac.2013.09.028.

Shastri V. P., Rahman N., Martin I., Langer R. (1998) Application of Conductive Polymers in Bone Regeneration. *MRS Proc* 550:215.
DOI: https://doi.org/10.1557/PROC-550-215.

Sood A., Gupta A., Agrawal G. (2021) Recent advances in polysaccharides based biomaterials for drug delivery and tissue engineering applications. *Carbohydr Polym Technol Appl* 2:100067.
DOI: https://doi.org/10.1016/J.CARPTA.2021.100067.

Tirgar M., Hosseini H., Jafari M., et al. (2021) Introducing a Flexible Drug Delivery System Based on Poly(Glycerol sebacate-Urethane) (PGS-U) and Its Nanocomposite: Potential Application in the Prevention and Treatment of Oral Diseases. *J Biomater Sci Polym Ed,* 1–17.
DOI: https://doi.org/10.1080/09205063.2021.1992588.

Venkatesan J., Kim S. K. (2014) Nano-hydroxyapatite composite biomaterials for bone tissue engineering - A review. *J. Biomed. Nanotechnol* 10:3124–3140.

Wang W., Zhang B., Li M., et al. (2021) 3D printing of PLA/n-HA composite scaffolds with customized mechanical properties and biological functions for bone tissue engineering. *Compos Part B Eng* 224:109192.
DOI: https://doi.org/10.1016/j.compositesb.2021.109192.

Wu Y., Chen Y. X., Yan J., et al. (2016) Fabrication of conductive gelatin methacrylate-polyaniline hydrogels. *Acta Biomater* 33:122–130.
DOI: https://doi.org/10.1016/j.actbio.2016.01.036.

Zhang Q., Song M., Xu Y., et al. (2021) Bio-based polyesters: Recent progress and future prospects. *Prog Polym Sci* 120:101430.
DOI: https://doi.org/10.1016/j.progpolymsci.2021.101430.

Zia K. M., Noreen A., Zuber M., et al. (2016) Recent developments and future prospects on bio-based polyesters derived from renewable resources: A review. *Int J Biol Macromol* 82:1028–1040.
DOI: https://doi.org/10.1016/J.IJBIOMAC.2015.10.040.